Electrosynthesis and Characterization of an Electrochromic Material from 2-(3-Thienyl)ethyl acrylate

Kaiwen Lin‡[1], Shimin Zhang‡[2], Hongtao Liu[1], Yao Zhao[1], Daize Mo[1], Jingkun Xu[1,]*

[1] Jiangxi Key Laboratory of Organic Chemistry, Jiangxi Science and Technology Normal University, Nanchang 330013, China
[2] Academy of Fundamental and Interdisciplinary Sciences, Harbin Institute of Technology, Harbin, 150001, China
[*]E-mail: xujingkun@tsinghua.org.cn
‡ *These authors contributed equally to this work.*

A novel acrylate modified 3-thienylethanol (TE) was synthesized and its electropolymerization led to the formation of corresponding acrylate modified poly(3-thienylethanol) (PTE-AA). The structure, redox activity, electrochemical stability, optical properties, thermal properties and morphology of obtained polymer were systematically studied *via* FT-IR, thermogravimetry, cyclic voltammetry and scanning electron microscopy (SEM). The FT-IR spectrum of polymer displayed that the polymerization occurred at the 2, 5-substituted position of the thiophene ring. PTE-AA exhibited good electrochemical stability with less obvious degradation only 10% after scanning 4000 cycles. The band gaps of the polymer was 2.21 eV calculated based on the spectroelectrochemistry analysis. In addition, electrochromic studies demonstrated that PTE-AA showed various colors with different applied potentials. The introduction of the acrylate group significantly improves the electrochromic properties of PTE and results in high coloration efficiency (168 cm^2 C^{-1}) and low switching voltage and fast response time (2.7 s).
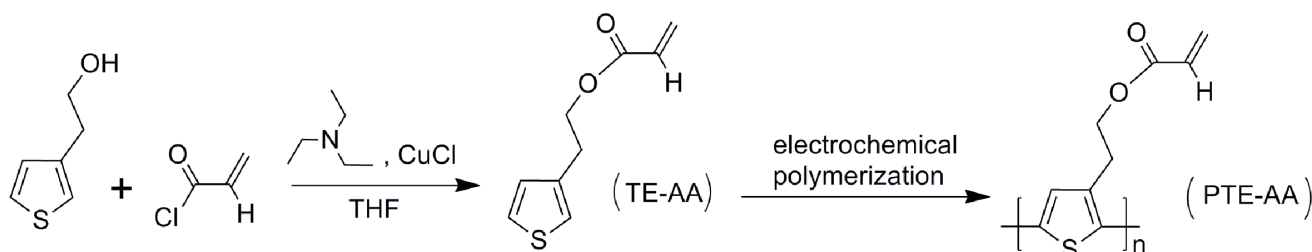
1. INTRODUCTION

Conducting polymers (CPs) continue and still to be a primary focus of optoelectronic materials to be utilized in electronic devices such as electrochromic devices (ECDs) [1], photovoltaics (PVs) [2], light emitting diodes (LEDs) [3] and field effect transistors (FETs) [4]. Among the conducting polymers, electrochromic (EC) polymers have been widely used in various devices due to their

excellent advantages such as low switching potential, high contrast ratio, electrochemical stability and ease of color control by structure modification [5-6].

As known, poly(thiophene) (PTh) and its derivatives have unique advantages such as low band gap, ease of synthesis and modification, high conductivity and high stability, *etc* [7]. As electrochromic materials, PTh and its derivatives also revealed many colors in redox states [8] and have been used for the synthesis of novel π-conjugated systems with excellent electrochromic performances. In addition, introduction of side groups into the main chain of polymer not only affect the oxidation potentials of monomers and polymers, solubility and the optical properties of the polymers but also could be used to introduce functional groups [9]. And 3-thiophene ethanol (TE), as a derivative of thiophene, has been used to synthesize different thiophene-based precursors with different functional groups via substitutions of hydroxyl group [10-12]. Furthermore, photo-cross-linkable acrylate group, for example poly(3,4-alkylenedioxythiophene)s with acrylate-function are processable in solution and patternable for large-area electrochromic films [13], has been found lately and interest us to investigate the field.

In this work, acrylate group was introduced to TE to form a precursor, and its electrochemical polymerization was studied, as shown in Scheme 1. The PTh with acrylate-function revealed amazing electrochromic properties, and our previous work [14] also showed that materials from 2'-methyl acrylate-3,4-ethylenedioxythiophene (EDOT-AA) which displayed good optoelectronic properties. More detailed description of PTE-AA and PEDOT-AA about their electropolymerization and optoelectronic properties were comparative studied in particular.

Scheme 1. Synthesis route for TE-AA and corresponding polymer.

2. EXPERIMENTAL

2.1 Materials.

3-Thienylethanol (TE) (98%; Energy) and acryloyl chloride (98%; Energy) were used without further treatment. Boron trifluoride diethyl etherate (BFEE) (Beijing Changyang Chemical Plant) was distilled before use. Tetrahydrofuran (THF) and dichloromethane (CH_2Cl_2, analytical grade) was used after reflux distillation. Other reagents and chemicals were purchased from Beijing East Longshun Chemical Plant (Beijing, China) and were used without any further treatment.

2.2 Synthesis of 2-(3-Thienyl)ethyl acrylate (TE-AA)

3-thienylethanol（4 g, 31.2 mmol）, 4.2 g (40.6 mmol) of distilled triethylamin, and a spot of CuCl were all dissolved in 30mL THF. Acryloyl chloride (3.68 g, 40.6 mmol) in 30mL of THF was added into above solution slowly at 0° C. At the temperature, the mixture was stirred for 2h. Then, we filtered the triethylammonium chloride by a silica gel column. After the solvent evaporation, a mixture of 1:1 CH_2Cl_2 and 2M NaOH was added and the mixture was stirred overnight. The organic layer was separated, washed twice with water, and dried over $MgSO_4$. After solvent evaporation, the remaining crude product was isolated by columnchromatography with silica (ethyl acetate/petroleum ether = 1/3, by volume) to give TE-AA as a colorless liquid (yield 75 %). ^1H NMR (400 MHz, $CDCl_3$): δ (ppm) 7.26 (m, 1H), 6.97-7.04 (m, 2H), 6.38-6.42 (m, 1H), 6.1 (m, 1H), 5.81 (m, 1H), 4.37 (t, 2H), 3.02 (t, 2H). ^{13}C NMR: δ 167.24, 138.05, 136.23, 128.23, 125.52, 121.51, 64.49, 29.51, 18.25. (Figure 1)

2.3 Electropolymerization

The electrochemical tests were investigated in a one-compartment cell using a potentiostat-galvanostat (model 263A, EG&G Princeton Applied Research) under computer control. An Ag/AgCl electrode directly immersed in the solution served as the reference electrode, and it revealed sufficient stability during the experiments. For electrochemical tests, the working and counter electrodes were both Pt wire with a diameter of 1 mm, respectively. To obtain a sufficient amount polymers, ITO or Pt were used as the working and counter electrodes, respectively. All the solutions were deaerated by a dry nitrogen stream for 20 min and maintained under a slight overpressure through all the experiments. After polymerization, the polymer films were washed repeatedly with anhydrous diethyl ether to remove the electrolyte and monomer.

2.4 Characterization

^1H NMR and ^{13}C NMR spectra were recorded on a Bruker AV 400 NMR spectrometer at ambient temperature. $CDCl_3$ was used as the conventional solvent and chemical shifts were recorded in ppm units with tetramethylsilane (TMS) as the internal standard. Fourier Transform Infrared spectra (IR) were determined with a Bruker Vertex 70 Fourier-transform infrared (FT-IR) spectrometer with samples in KBr pellets. Thermogravimetric analysis (TGA) was studied with a Pyris Diamond TG/DTA thermal analyzer (PerkinElmer) under a nitrogen stream from 290 to 1100 K at a heating rate of 10 K min^{-1}. Scanning electron microscopy (SEM) measurements were made by using a VEGA II-LSU scanning electron microscope (Tescan) with the polymer films deposited on the ITO-coated glass.

2.5 Electrochromic experiments

Spectroelectrochemical and kinetic studies were carried out on a Model 263 potentiostat-galvanostat (EG&G Princeton Applied Research) and a Specord 200 Plus (Analytikjena)

spectrophotometer at a scan rate of 2000 nm min^{-1} under computer control. The spectroelectrochemical cell consists of a quartz cell, an Ag wire, a Pt wire, and an ITO/glass as transparent working electrode. All measurements were carried out in the mixture of CH$_2$Cl$_2$-BFEE (1:1, by volume). The optical density (ΔOD) at the specific wavelength (λ_{max}) was determined by using the optical contrast values ($\Delta T\%$) of the electrochemically oxidized and reduced films, using the following equation: [15]

$$\Delta OD = log(T_{ox}/T_{red}) \qquad\qquad (1)$$

The coloration efficiency (*CE*) is defined as the relation between the injected/ejected charge as a function of electrode area (Q_d) and the change in optical density (ΔOD) at the specific wavelength (λ_{max}) as illustrated by the following equation: [16]

$$CE = \Delta OD/Q_d \qquad\qquad (2)$$

3. RESULT AND DISCUSSION

3.1 Monomer synthesis

The target compound was synthesized as shown in Scheme 1. The reagents, 3-thienylethanol, triethylamin, acryloyl chloride and CuCl were all purchased from Energy Chemical. The targeted compound was synthesized via CuCl catalytic coupling reaction in satisfactory yield. The ^{1}H NMR and ^{13}C NMR spectra of the monomer were studied, as shown in Figure 1. ^{1}H NMR (400 MHz, CDCl$_3$): δ (ppm) 7.26 (m, 1H), 6.97-7.04 (m, 2H), 6.38-6.42 (m, 1H), 6.1 (m, 1H), 5.81 (m, 1H), 4.37 (t, 2H), 3.02 (t, 2H). ^{13}C NMR: δ 167.24, 138.05, 136.23, 128.23, 125.52, 121.51, 64.49, 29.51, 18.25. (Figure 1)
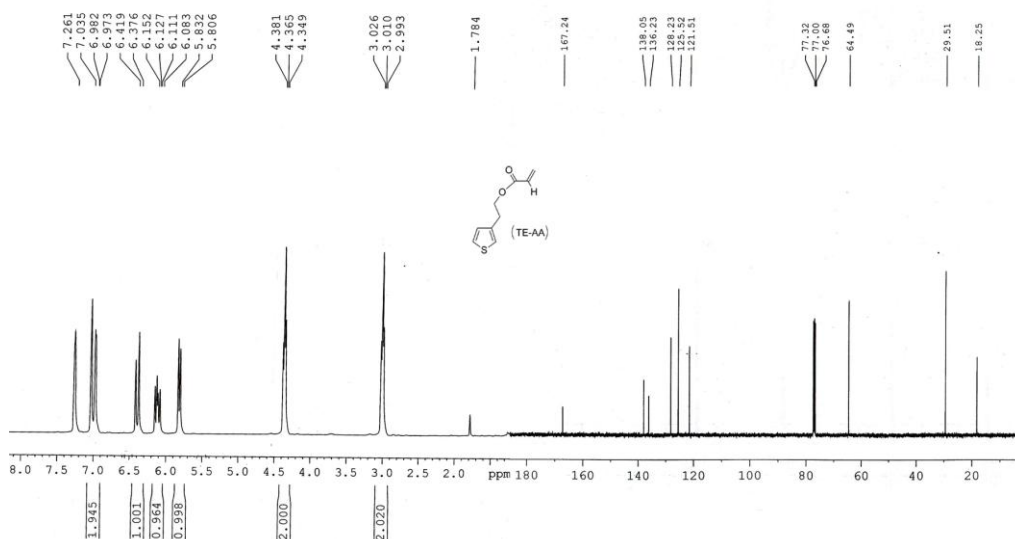

Figure 1. ^{1}H NMR and ^{13}C NMR spectra of the monomer in CDCl$_3$.

3.2 Cyclic voltammetry

Cyclic voltammetry (CV) is a very useful method to reveal the reversibility of electron transfer during the electropolymerization and to examine the electroactivity of the polymer film because the oxidation and reduction can be monitored in the form of a current-potential diagram [17]. Combining the facile electrosynthesis of high-quality polymer films in BFEE and the good solubility of the

monomer in solvent CH_2Cl_2, a solvent electrolyte containing 50% (vol) BFEE and 50% (vol) CH_2Cl_2 was chosen as the electrolyte system.
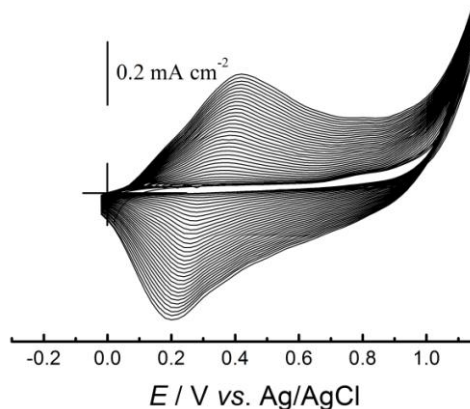

Figure 2. CVs of TE-AA in CH_2Cl_2-BFEE (1:1, by volume). Monomer concentration: 10 mmol L^{-1}.

Figure 2 shows the cyclic voltammograms (CVs) of TE-AA in CH_2Cl_2-BFEE (1:1, by volume). The figure showed characteristic features of typical conducting polymers during potentiodynamic synthesis, which was also in agreement with thiophene and alkylthiophenes [18]. From Figure 1, we can found the onset oxidation potentials was found at 0.99 V for TE-AA which was approximately 0.26 V lower than that of EDOT-AA (near 1.25 V). This indicated that PTE-AA can be easily obtained *via* electrochemical polymerization. In addition, the oxidation and reduction peaks were observed at 0.42 and 0.20 V for PTE-AA, exhibiting an obvious redox activity.

Moreover, the increases of the redox wave currents indicated that the amount of the polymer film was increasing on the electrode surface with CV proceeding. The broad redox waves may be due to the wide distribution of chain length or the conversion of conductive species on polymer main chain from the neutral state to the metallic state [19].

3.3 Optimization of electrical conditions and preparation of polymers
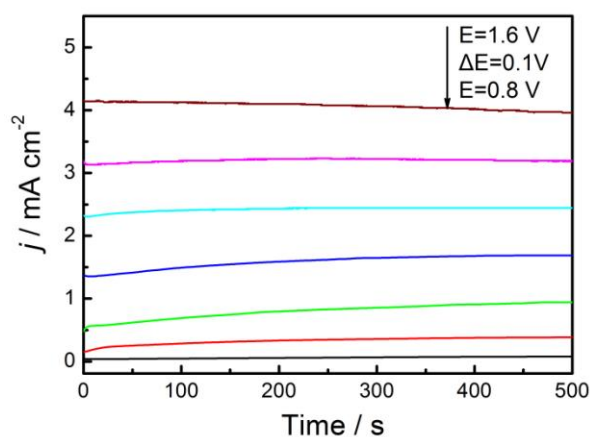

Figure 3. Chronoamperograms of 10 mmol L^{-1} TE-AA in CH_2Cl_2-BFEE (1:1, by volume) on Pt electrode at different applied potentials for 500 s.

Potentiostatic electropolymerization was used to prepare the polymer films. To optimize the electropolymerization condition, a set of current transients at different applied potentials were recorded, as shown in Figure 3. Typically, when the applied potentials below the onset oxidation potential, there was no polymer film was formed on the electrode. Once the potential ran up to the critical value, the current densities initially undergo a sharp increased and then a slightly decreased and finally kept constant because of uniform electropolymerization of the polymer film. However, at relatively high potentials, the surfaces of the polymer film revealed half-baked and heterogeneous. This phenomenon was mainly because of the overoxidation, which led to poor quality films [20]. Therefore, PTE-AA used for the characterization mentioned below was prepared at constant potentials of 1.20 V.
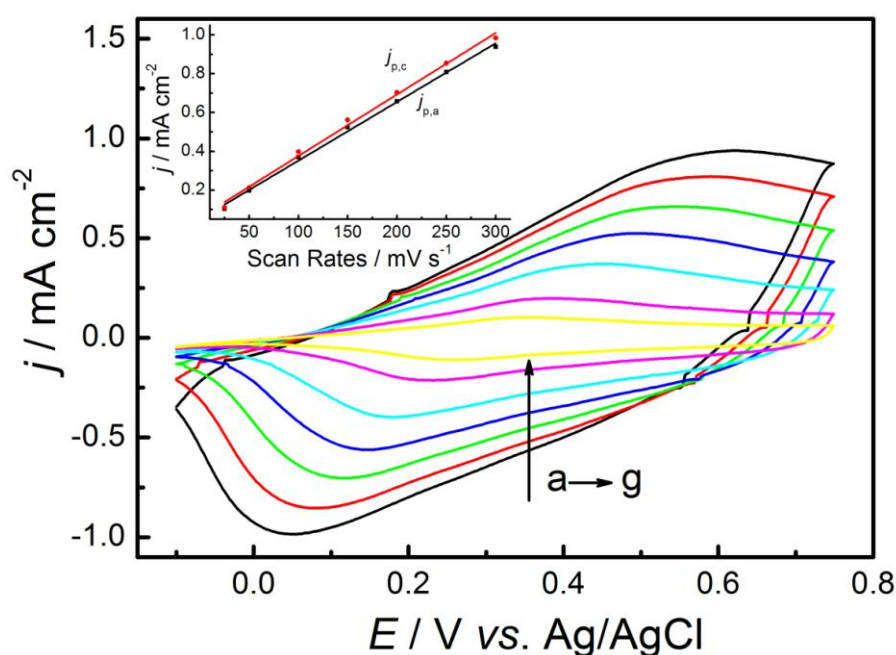
3.4 Electrochemistry of polymer films

Figure 4. CVs of PTE-AA in CH_2Cl_2-BFEE (1:1, by volume) at potential scan rates of (a) 300 mV s^{-1}, (b) 250 mV s^{-1}, (c) 200 mV s^{-1}, (d) 150 mV s^{-1}, (e) 100 mV s^{-1}, (f) 50 mV s^{-1} and (g) 25 mV s^{-1}. Inset: plots of redox peak current densities *vs.* potential scan rates. j_p is the peak current density: and $j_{p,a}$ and $j_{p,c}$ denote the anodic and cathodic peak current densities, respectively.

In order to test the electroactivity and stability of the obtained polymer films, cyclic voltammetry was empolyed in monomer-free CH_2Cl_2-BFEE, as shown in Figure 4. The CVs at different potential scan rates illustrated broad redox peaks similar to those of polythiophene [21]. The peak current densities were proportional to the potential scanning rates (inset), showing that electroactive monomer was well adhered to the working electrode and the redox process is nondiffusional.

3.5 Structural characterization

FT-IR spectra of monomer and the dedoped polymer were recorded to investigate the structure of polymers, as shown in Figure 5. Similar to other reported conjugated polymers previously [22], the absorption bands of the polymer were obviously broadened compared to the monomer. This mainly owing to the wide chain dispersity of the as-formed polymer film composed of oligomers/polymers [23].
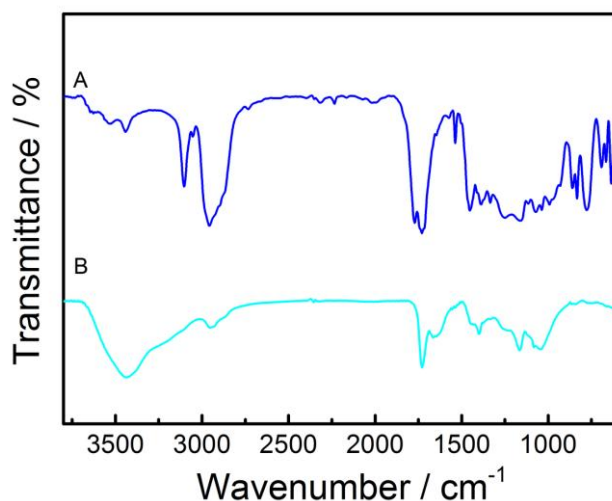

Figure 5. FT-IR spectra of TE-AA (A) and PTE-AA (B).

Peaks located in the range of 2864 to 2930 cm^{-1} correspond to the CH_2 vibrations and were present in monomer and polymer. The large peak at 1725 cm^{-1} was due to the carbonyl stretching vibrations in monomer and polymer and the C=C stretching vibration frequency at 1637 cm^{-1} appeared in TE-AA, approximately at the same region as that for PTE-AA, indicating that the acrylate group was not destroyed during the electrochemical polymerization. Furthermore, the bands of PTE-AA owning to C-H stretching of thiophene at about 3105 cm^{-1} in the monomer spectra was nearly absent or weak, indicating the occur of electrochemical polymerization at the thiophene rings. In the fingerprint region, the emergence of 860 cm^{-1} might be due to the out-of-plane bending vibration of adjacent C-H in the thiophene ring. This confirmed that the polymerization occured primarily at α-positions, namely, $C_{(2)}$ and $C_{(5)}$ positions of thiophene, which agreed with previous reports [24].

3.6 Thermal Analysis

Thermogravimetric analytical tests were investigated under a nitrogen stream at a heating rate of 10 K min^{-1} to explore the thermal stability of the polymers, as shown in Figure 6. It can be syllabify observed that the obtained polymer underwent a slightly weight decrease about 6.2% at relatively low temperature (from 290 K to 650 K), which may be due to a few monomer trapped in the polymer and water evaporation [25]. With the increase of the temperature, a more prominent weight loss step was

found at 650 K < T < 800 K. This prominent weight loss was mainly because of the oxidizing decomposition of the skeletal backbone chain. To be more specific, because of acrylate group, polymer was easily to crack and decompose the chain length of the polymer film. The following degradation after 800 K was possibly as a result of the overflow of monomer decomposed from polymer. When the temperature mounted into about 1100 K, the residue of PTE-AA was about 57.6%, which displayed lower degradation rate compared with its heteroanalogue PEDOT-AA with the residue about 36.1% [14].
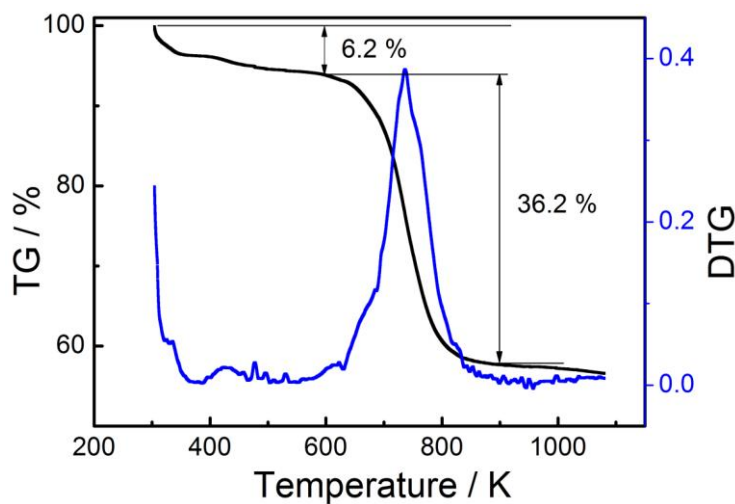

Figure 6. TG/DTG curves of dedoped PTE-AA film.
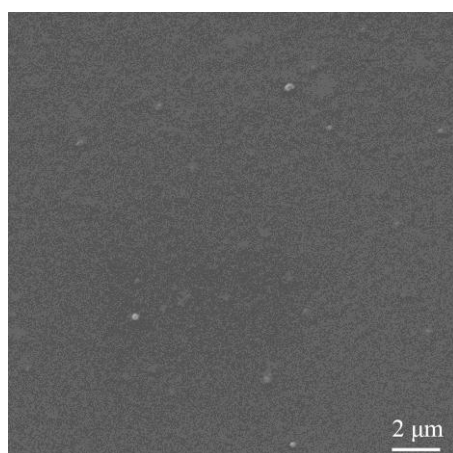
3.7 Morphology

Figure 7. SEM of PTE-AA film electrodeposited on ITO electrode.

Scanning electron micrographs (SEM) of polymer reveal their surface topography and bulk morphologies, which are two important aspects relevant to their photoelectric properties, such as

charge transport and counterions storage capability. Figure 7 display the morphology of polymer films. It is noticed that the morphological structure of PTE-AA show smooth and homogeneous surface. The homogeneous and compact morphology of obtained polymer film was profitable for improving the performances, such as electron transfer capacity, electrical conductivity and electrochromic performances [14].

3.8 Spectroelectrochemistry

In order to obtain the electronic structure of PTE-AA and to investigate the spectral changes during the redox process, spectroelectrochemistry of corresponding polymer film was studied, as shown in Figure 7. PTE-AA was prepared at 1.20 V *vs.* Ag/AgCl and was switched between -1.0 and +1.0 V.
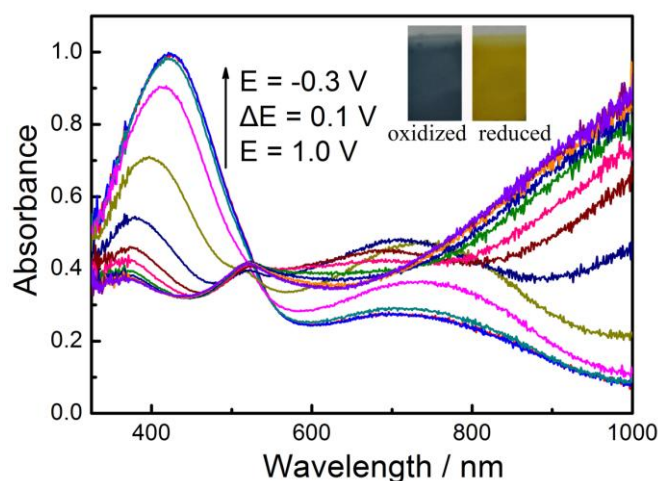

Figure 8. Spectroelectrochemistry for PTE-AA on ITO coated glass in CH_2Cl_2-BFEE (1:1).

In the neutral state, the UV-vis absorption of polymer films showed strong absorption peaks in the visible regime at 420 nm due to the π-π* transition. With the applied potential increasing, the peak of π-π* transition decreased while the evolution of new absorption bands with a width from 600 nm to 900 nm was observed. This typically represented the polaron charge carrier bands along the polymer backbone. Upon further oxidation of the polymer films, appearance of absorptions at longer wavelength (>900nm) was observed, which mainly due to the formation of bipolaron charge carriers [26]. The bandgaps (E_g), defined as the onset of the π-π* transition, was determined as 2.21 eV for PTE-AA, causing the films to appear in various degrees of yellow, as shown in photographs from insets of Figure 8. The PTE-AA films at oxidized states showed blackish green. For a comparative study, the color of PEDOT-AA was transmissive blue in the oxidized state and dark brown in the reduced state. The optical band gap of PEDOT-AA was about 1.64 eV, lower than that of PTE-AA (2.21 eV) [14].

3.9 Electrochromic switching of polymer films

It is significant that a polymer can reveal color changes and switch rapidly during redox process [27]. Optical contrast, an important characteristic of electrochromism, is defined as the transmittance difference between the redox states [28]. As can be seen from Figure 9, the optical contrast of PTE-AA at 900 and 420 nm were found to be 34.9% and 26.2%. Response time was calculated at 95% of the full switch [29]. The optical response time of PTE-AA were found to be 1.1 s from the oxidized to the reduced state and 1.3 s from the reduced to the oxidized state at 420 nm, which is faster than that of the structurally similar PEDOT-MA reported in literature [14]. The response time from oxidized to reduced is faster than that from reduced to oxidized state. This phenomenon was mainly due to the ease of charge transport when it is reduced. The coloration efficiency of PTE-AA film was determined to be 153.5 cm^2 C^{-1} at 420 nm and 168 cm^2 C^{-1} at 900 nm. In comparison, the optical contrast and coloration efficiency of PTE-AA were lower than that of PEDOT-MA at different wavelength. Furthermore, coloration efficiency, response time and the optical contrast of polymer film were summarized in Table 1.
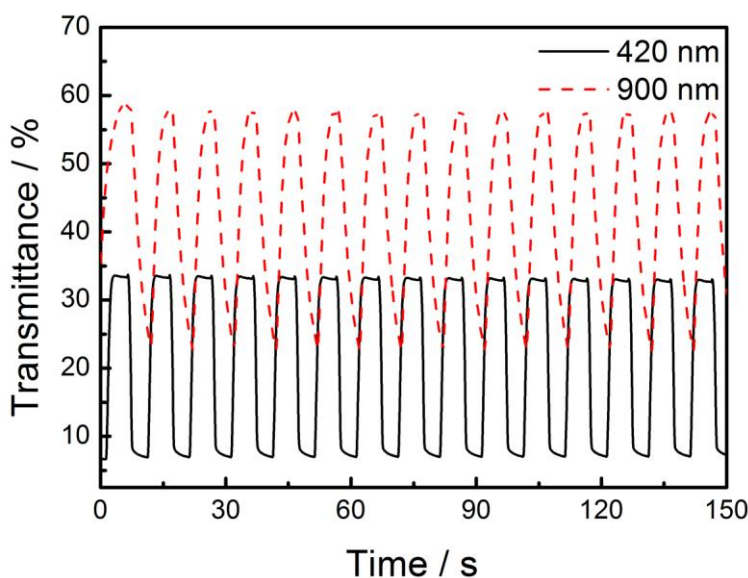

Figure 9. Electrochromic switching and optical absorbance monitored at primary wavelength for PTE-AA recorded during double step spectrochronoamperometry.

Table 1. Optical properties for polymer film

polymers	Wavelength/nm	potential step/V	ΔT/%	response time (s) oxidation	response time (s) reduction	CE (cm^2/C)	λ/nm Abs. max	λ/nm Abs. onset	E_g^a/eV
PTE-AA	420 900	-1.0~1.0	26.2 34.9	1.3 4.5	1.1 2.7	153.5 168.0	420	560	2.21

[a] The date were calculated by the equation: $E_g = 1241/\lambda_{onset}$ of polymer film.
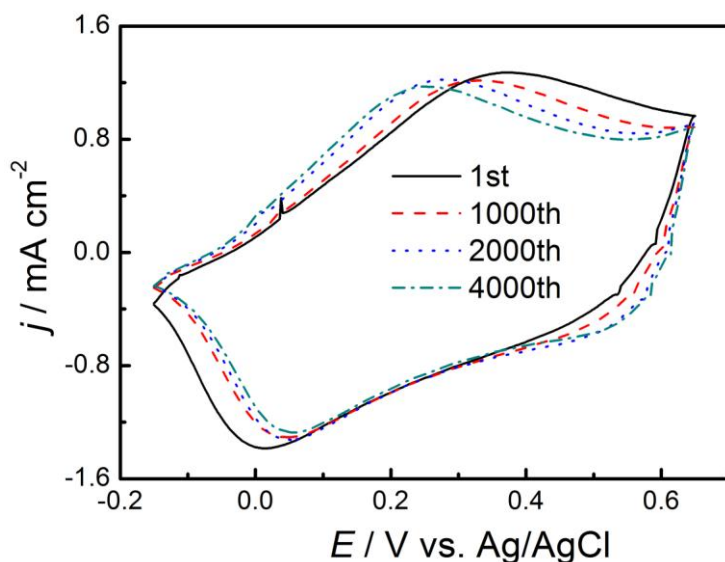
3.10 Stability of of PTE-AA

Figure 10. Long-term CVs of PTE-AA in CH_2Cl_2-BFEE (1:1, by volume) upon repeated cycling at the scan rate of 150 mV s^{-1}.

As is known to all, electrochemical stability of conducting polymer is important for its application in organic devices [30]. Therefore, the electrochemical stability of PTE-AA was studied in monomer-free CH_2Cl_2-BFEE (1:1, by volume) solution, as shown in Figure 10. During the redox process of PTE-AA, 90% of its electroactivity is retained after 4000 cycles. The result indicated that PTE-AA had fine redox stability, and its long lifetimes meant PTE-AA had good effective charge compensation ability.

4. CONCLUSION

In conclusion, acrylate functionalized TE-AA was synthesized, and its corresponding polymer PTE-AA was also electrosynthesis under optical conditions. As formed polymer film PTE-AA showed good redox activity and long-term stability in monomer-free CH_2Cl_2-BFEE, and smooth and compact morphology. Spectroelectrochemistry revealed that PTE-AA film had distinct electrochromic properties and showed yellow at neutral state and blackish green at full oxidized state. Maximum contrast ($\Delta T\%$) at primary wavelength and response time of the PTE-AA film were measured as 26.2% and 1.1 s at 420 nm, respectively. The *CE* was calculated to be 153.5 cm^2 C^{-1}. These properties make PTE-AA a good candidate for commercial applications.

References

1. C. Pozo-Gonzalo, M. Salsamendi, A. Vinuales, J.A. Pomposo, H.J. Grande, *Sol. Energy Mater. Sol. Cells.* 93 (2009) 2093–2097.
2. A.P. Zoombelt, M. Fonrodona, M.G.R. Turbiez, M.M. Wienk, R.A.J. Janssen, *J. Mater. Chem.* 19 (2009) 5336–5342.
3. A. Garcia, R.C. Bakus, P. Zalar, C.V. Hoven, J.Z. Brzezinski, T.Q. Nguyen, *J. Am. Chem. Soc.* 133 (2011) 2492–2498.
4. P.M. Beaujuge, W. Pisula, H.N. Tsao, S. Ellinger, K. Müllen, J.R. Reynolds, *J. Am. Chem. Soc.* 131 (2009) 7514–7515.
5. B. Yigitsoy, S.M.A. Karim, B. Balan, D. Baran, L. Toppare, *Synth. Met.* 160 (2010) 2534–2539.
6. A.L. Dyer, M.R. Craig, J.E. Babiarz, K. Kiyak, J.R. Reynolds, *Macromolecules* 43 (2010) 4460–4467.
7. Y. H. Pang, H. Xu, X. Y. Li, *Electrochem. Commun.* 8 (2006) 1757–1761.
8. S. Thomas, C. Zhang, S. S. Sun, *J. Poly. Sci. A: Poly. Chem.* 43 (2005) 4280–4289.
9. W.J.D. III, R.J. Wysocki, N.R. Armstrong, S.R. Saavedra, *Macromolecules* 39 (2006) 4418–4424.
10. P.J. Costanzo, K.K. Stokes, *Macromolecules* 35 (2002) 6804–6810.
11. P. Camurlu, A. Cirpan, L. Toppare, *Synth. Met.* 146 (2004) 91–97.
12. L. Sacan, A. Cirpan, P. Camurlu, L. Toppare, *Synth. Met.* 156 (2006) 190–195.
13. J. Kim, J. You, B. Kim, T. Park, E. Kim, *Adv. Mater.* 23 (2011) 4168–4173.
14. L.Q. Qin, J.K. Xu B.Y. Lu, Y. Lu, X.M. Duan, G.M. Nie, *J. Mater. Chem.* 22 (2012) 18345–18353.
15. G. Sonmez, *Chem. Commun.* (2005) 5251–5259.
16. H. Zhou, L. Yang, S.C. Price, K. J. Knight, W. You, *Angew. Chem. Int. Ed.* 122 (2010) 8164–8167.
17. X.G. Li, M.R. Huang, W. Duan, Y.L. Yang, *Chem. Rev.* 102 (2002) 2925–3030.
18. P. Tschuncky, J. Heinze, *Synth. Met.* 1603 (1993) 55–57.
19. B. Wang, J.S. Zhao, J. Xiao, C.S. Cui, R.M. Liu, *Int. J. Electrochem. Sci.* 7 (2012) 2781–2795
20. B. Y. Lu, S. J. Zhen, S. M. Zhang, J. K. Xu, G. Q. Zhao, *Polym. Chem.* 5 (2014) 4896–4908.
21. J. Roncali, F. Garnier, *Synth. Met.* 15 (1986) 323–331.
22. J. K. Xu, J. Hou, S. S. Zhang, G. M. Nie, S. Z. Pu, L. Shen, Q. Xiao, *J. Electroanal. Chem.* 578 (2005) 345–355.
23. B. Y. Lu, J. Yan, J. K. Xu, S. Y. Zhou, X. J. Hu, *Macromolecules* 43 (2010) 4599–4608.
24. K.W. Lin, S.J. Zhen, S.L. Ming, J.K. Xu, B.Y. Lu, *New J. Chem.* 39 (2015) 2096–2105.
25. J. C. Thieblemont, A. Brun, J. Marty, M. F. Planche, P. Calo, *Polymer* 36 (1995) 1605–1612.
26. P. Camurlu, A. Cirpan, L. Toppare, *Mater. Chem. Phys.* 92 (2005) 413–418.
27. G.M. Nie, L.J. Zhou, Q.F. Guo, S.S. Zhang, *Electrochem. Commun.* 12 (2010) 160–168.
28. J.S. Zhao1, X.F. Cheng, Y.Z. Fu, C.S. Cui, *Int. J. Electrochem. Sci.* 8 (2013) 1002–1015
29. A. Cihaner, F. Algı, *Electrochim. Acta.* 54 (2008) 786–792.
30. F. Uckert, Y. H. Tak, K. Müllen, H. Bässler, *Adv. Mater.* 12 (2000) 905–908.